



HAL
open science

Numerical investigation of the effects of heating and contact conditions on the thermal charging performance of composite phase change material

Xusheng Hu, Feng Zhu, Xiao-Lu Gong

► **To cite this version:**

Xusheng Hu, Feng Zhu, Xiao-Lu Gong. Numerical investigation of the effects of heating and contact conditions on the thermal charging performance of composite phase change material. *Journal of Energy Storage*, 2020, 30, pp.101444. 10.1016/j.est.2020.101444 . hal-02626589v2

HAL Id: hal-02626589

<https://utt.hal.science/hal-02626589v2>

Submitted on 3 Jun 2022

HAL is a multi-disciplinary open access archive for the deposit and dissemination of scientific research documents, whether they are published or not. The documents may come from teaching and research institutions in France or abroad, or from public or private research centers.

L'archive ouverte pluridisciplinaire **HAL**, est destinée au dépôt et à la diffusion de documents scientifiques de niveau recherche, publiés ou non, émanant des établissements d'enseignement et de recherche français ou étrangers, des laboratoires publics ou privés.



Distributed under a Creative Commons Attribution - NonCommercial 4.0 International License

Numerical investigation of the effects of heating and contact conditions on the thermal charging performance of composite phase change material

Xusheng Hu^a, Feng Zhu^{a,b}, Xiaolu Gong^{a,*}

^aCharles Delaunay Institute, LASMIS, University of Technology of Troyes, 12 Rue Marie Curie, 10004 Troyes, France

^bInstitute of electrical engineering, Chinese academy of sciences, Beijing 100190, China

(*) Correspondent author, gong@utt.fr

Abstract

Phase change material (PCM) saturated in metal foam is a promising candidate for thermal energy storage (TES). However, there are some potential factors affecting the thermal charging performance of composite PCM, such as heating and contact conditions. In this paper, paraffin and copper foam are selected as PCM and metal matrix, respectively. Heating conditions are top, left and bottom heating. The contact gaps are set to 0, 0.4 and 0.8 mm to represent different contact conditions. The numerical investigation on thermal charging performance of composite PCM under different heating and contact conditions is performed. Based on volume-averaged method, the numerical model is developed to study the thermal characteristics of composite PCM including solid-liquid interface, liquid fraction, velocity, total melting time and average heat storage rate. Results show that there are the comprehensive effects of heating and contact conditions on thermal performance. The heating condition can affect phase change heat transfer mode, and thus has a significant influence on thermal charging performance. The contact conditions have the different effects on thermal behavior of composite under different heating conditions, e.g., under top heating condition, the total melting time of composite with 0 mm and 0.8 mm contact gap is almost the same. Whereas, under left heating condition, the total melting time of composite with 0.8 mm contact gap is 2.6 times that of composite with 0 mm contact gap. The study of the effect mechanism of heating and contact conditions is of great significance for practical application of composite PCM in TES system.

Keywords: Metal foam, Phase change material, Heating and contact conditions, Numerical simulation, Volume-average method

Nomenclature			
A_m	mush constant	Greek symbols	
B	correlation coefficient	β	liquid fraction within pore
C	inertial coefficient (1/m)	γ	thermal expansion coefficient (1/K)
c	specific heat capacity (J/kg K)	ε	porosity of metal foam
g	gravitational acceleration (m/s ²)	λ	small constant
K	permeability (m ²)	μ	dynamic viscosity (kg/m s)
k	thermal conductivity (W/m K)	ρ	density of material (kg/m ³)
L	latent heat (J/kg)	φ	liquid fraction of entire composite
p	pressure (Pa)	Subscripts	
S	source term	eff	effective
T	temperature (K)	f	phase change material
T_{m1}	solidus temperature (K)	i	initial
T_{m2}	liquidus temperature (K)	s	metal foam
t	time (s)	w	wall
u,v	velocity in x and y direction (m/s)		

1. Introduction

With the rapid development of human society and economy, environment pollution and energy issue are becoming more and more serious in recent years. Researchers pay extensive attention to the development of renewable energy resources [1], in which thermal energy storage (TES) plays an important role in energy storage and release [2, 3]. Due to the high energy storage density and good thermal stability, phase change materials (PCMs) are widely used in TES system [4], such as solar thermal power plant [5], energy efficient building [6] and waste heat recovery system [7]. However, the relatively lower thermal conductivity hinders widespread utilization of PCMs in TES system. To enhance the thermal behavior of PCM, some methods have been studied, which include encapsulated PCMs [8, 9], adding high thermal conductivity additive [10, 11], inserting metal matrix and pin-fin [12, 13], and embedding metal foam [14-16]. A mass of investigations demonstrated that embedding metal foam can effectively heighten the thermal behavior of PCM.

Yang et al. [17, 18] carried out the numerical studies of the role of metal foam on the enhancement in thermal behavior of TES system using PCM. Results proved that embedding metal foam can significantly enhance the thermal behavior of TES unit and the uniformity of temperature was also improved. Xiao et al. [19, 20] prepared the paraffin/metal foam composite PCMs and experimentally investigated the thermal characteristics of composite PCMs, especially effective thermal conductivity. Lafdi et al. [21] investigated the effects of porosity and pore density on the thermal behavior of PCM saturated in aluminum foam using the experimental approach. The numerical and experimental investigations on phase change process of PCMs impregnated in graded porosity metal foam were performed in [22, 23]. Effect of orientation of copper foam embedded in PCM on thermal performance was experimentally examined by Baby and Balaji [24]. The visual experiments of phase transition process were designed to analyze the thermal characteristic of paraffin/copper foam

composites [25, 26], where the local thermal non-equilibrium problem between the metal ligament and PCM was emphatically studied. Boomsma and Poulikakos [27] proposed the tetrakaidecahedron model taking into account the intricate configuration of metal foam. Feng et al. [28] performed the pore-scale and volume-average numerical simulation. They found that two numerical models have similar predictions and one-temperature volume-average model can be employed to imitate composite PCMs. It can be concluded from the above literature that most studies of metal foam/paraffin composite PCM mainly focus on the following aspects: the preparation of composite PCM, heat transfer mechanism, development of theoretical model and effects of configuration parameters (e.g. porosity, pore size and porosity gradient) on thermal behavior of composite PCMs.

Yataganbaba and Kurtbas [29] conducted an experimental investigation of the effects of heating positions and embedding metal foam on the thermal performance of pure PCM. Results showed that heating positions significantly affected the melting rate and temperature response of pure paraffin and melting of PCM was heightened by embedding metal foam. For real applications of composite PCM, such as solar thermal storage and thermal management of electronic devices, heating positions are different, which may affect its thermal performance. Moreover, for the same TES device, the studies of heating condition are also very necessary and significant. For instance, the heating position may have an important influence on the energy storage rate of composite PCM used in TES. However, the study on the effect of heating condition on the thermal performance of composite PCM is not enough.

In practical utilization, PCM needs to be encapsulated in containers [30]. The junction types between metal foam and container wall can result in the difference of contact condition. We should select the natural contact or bonding metal foam to the wall via sintering or brazing, which is still an open question. Hence, the effect of contact condition on thermal behavior of composite PCM employed in TES should be particularly investigated, which is conducive to determining which kind of the junction type is chosen to achieve high heat storage rate in a real application. To this end, the aim of this paper is to investigate the effects of heating and contact conditions on thermal charging performance for composite PCM. Based on the volume-average method, numerical simulation is implemented to investigate thermal characteristics of composite PCMs during the phase transition process, including solid-liquid interface, velocity, liquid fraction, melting time and heat storage rate. Nine different conditions are established to investigate the melting evolvement and heat transfer mechanism of composite PCMs subjected to different heating and contact conditions.

2. Problem description

Fig.1 presents the common contact condition of composite PCM used in TES. To easily assemble, there may be a small clearance fit between metal foam and wall. A contact gap of the width of δ yields between metal skeleton and container wall. The gap can be filled with PCM due to the flow of liquid PCM. The additional thermal resistance caused by the gap may have an effect on thermal behavior of composite PCM. Actually, due to different processing and assembly processes, the gap may occur in each pair of contact surfaces (i.e. top, bottom and sides). Besides, the heating condition also plays a vital role in the energy storage of composite PCM.

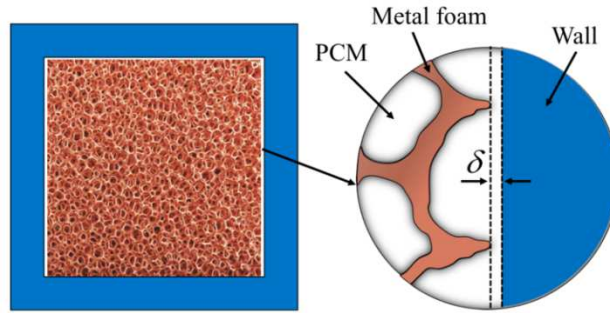


Fig. 1. Schematic diagram of contact condition of composite PCM for TES

To investigate the comprehensive effects of heating and contact conditions on the thermal performance of composite PCM, nine different heating and contact condition models are developed, as displayed in Fig. 2. For instance, Conds. 1, 4 and 7 are used for investigating the effect of heating position (blue wall is heated at a constant temperature, and grey represents PCM), and Conds. 4-6 are employed to study the influence of contact condition on thermal performance when heating condition is the same. The dimension of metal foam is the same (i.e. $50 \times 50 \text{ mm}^2$) for the nine different cases, in which foam is filled with PCM. The contact gaps with size of 0, 0.4 and 0.8 mm are set to represent different contact conditions. Since copper foam possesses not only high thermal conductivity but also large specific area, copper foam with 95% porosity and 5 PPI pore density is selected as metal matrix. Paraffin has the ability to store a large amount of heat by latent heat and is widely applied in TES, so it is used as PCM in this paper. The thermophysical properties of paraffin and copper foam are displayed in Table 1.

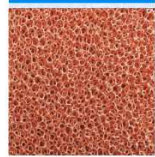
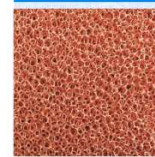
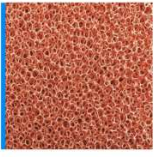
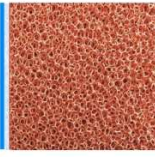
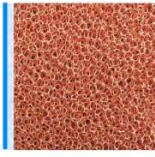
	$\delta=0 \text{ mm}$	$\delta=0.4 \text{ mm}$	$\delta=0.8 \text{ mm}$
Top	 Cond. 1	 Cond. 2	 Cond. 3
Left	 Cond. 4	 Cond. 5	 Cond. 6
Bottom	 Cond. 7	 Cond. 8	 Cond. 9

Fig. 2. Different heating and contact conditions

Table 1

Thermophysical properties of materials

Parameters	Materials	
	Paraffin	Copper foam
c (J/kg K)	2300	386
ρ (kg/m ³)	900	8900
k (W/m K)	0.3	380
μ (kg/m s)	0.00324	
γ (1/K)	0.0005	
L (J/kg)	148800	
T_{m1} (K)	323	
T_{m2} (K)	331	

3. Numerical simulation

3.1 Physical model

The computational domain of composite PCM is simplified to a two-dimensional model employed for the volume-averaged simulation. Fig. 3 presents the schematic diagram of physical model with the left heating condition. A square computational domain with size of $50 \times 50 \text{ mm}^2$ is used to represent the composite PCM, in which PCM is saturated in metal foam. The bad contact condition is considered (i.e. there is a gap with the width of δ between hot wall and composite PCM) to investigate the effect of contact condition, and we assume that the gap is completely filled with paraffin wax. The hot wall is heated with the fixed temperature $T_w = 350 \text{ K}$. The other walls are set to be adiabatic. The initial temperature of model is $T_i = 298 \text{ K}$.

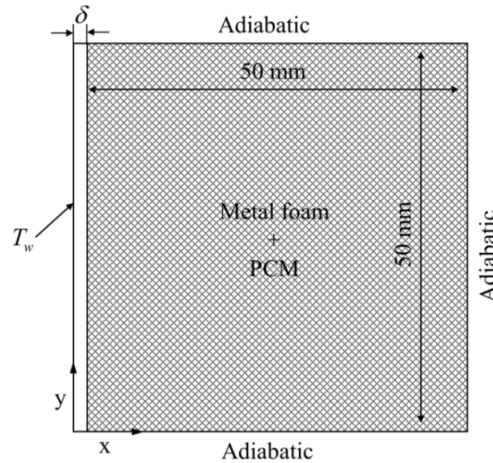


Fig. 3. Physical model of composite PCM

3.2 Mathematical method

The necessary assumptions should be made in mathematical method for the present physical model, as follows: (1) Metal foam is assumed to be homogenous and isotropic; (2) the flow of fusion paraffin within metal foam is treated as incompressible and Newtonian; (3) The thermal property of paraffin is considered as constant and same at solid and liquid state,

except density which is subject to the Boussinesq approximation.

The volume-averaged method is employed to simulate phase change process within composite PCM. Based on the assumption of local thermal equilibrium, one-temperature energy model is used to solve heat transfer between PCM and metal skeleton. Darcy-Brinkman-Forchheimer model is employed for considering influences of metal foam on the flow of fusion PCM. According to the above assumptions and method, the volume-averaged governing equations can be given by as follows:

Continuity equation:

$$\frac{\partial \rho_f}{\partial t} + \nabla \cdot (\rho_f \vec{U}) = 0 \quad (1)$$

Momentum equations

$$\frac{\rho_f}{\varphi} \frac{\partial u}{\partial t} + \frac{\rho_f}{\varphi^2} (\vec{U} \cdot \nabla) u = -\frac{\partial p_f}{\partial x} + \frac{\mu}{\varphi} \nabla^2 u - \left(\frac{\mu}{K} + \frac{C \rho_f |\vec{U}|}{\sqrt{K}} \right) u + S u \quad (2)$$

$$\frac{\rho_f}{\varphi} \frac{\partial v}{\partial t} + \frac{\rho_f}{\varphi^2} (\vec{U} \cdot \nabla) v = -\frac{\partial p_f}{\partial y} + \frac{\mu}{\varphi} \nabla^2 v - \left(\frac{\mu}{K} + \frac{C \rho_f |\vec{U}|}{\sqrt{K}} \right) v + \rho_f g \gamma (T - T_m) + S v \quad (3)$$

The term S in Eqs. (2) and (3) is the source term of damping force, and defined as the following equations [31]:

$$S = -\frac{(1-\beta)^2}{\beta^3 + \lambda} A_m$$

(4)

Where A_m is a mushy zone constant and set as 10^5 . λ is a small constant and set at 10^{-3} . β is the liquid fraction within the pore and defined by:

$$\beta = \begin{cases} 0 & T < T_{m1} \\ (T - T_{m1}) / (T_{m2} - T_{m1}) & T_{m1} < T < T_{m2} \\ 1 & T > T_{m2} \end{cases} \quad (5)$$

The relationship between β and φ can be written as:

$$\varphi = \varepsilon \cdot \beta \quad (6)$$

Energy equation for PCM and metal foam:

$$\frac{\partial T}{\partial t} [\varepsilon \rho_f c_f + (1-\varepsilon) \rho_s c_s] + \varepsilon \rho_f c_f (\vec{U} \cdot \nabla) T = k_{eff} \nabla^2 T - \varepsilon \rho_f L \frac{\partial \beta}{\partial t} \quad (7)$$

The pore size d_p can be determined by:

$$d_p = \frac{22.4 \times 10^{-3}}{\omega} \quad (8)$$

The permeability K and inertial coefficient C are required for the calculation of liquid flow within porous medium, which are complex parameters and difficult to be obtained by the experimental test. K and C are finally determined by using the model proposed in Ref. [32]

and written by the following equations:

$$\frac{K}{d_p^2} = 0.00073(1-\varepsilon)^{-0.224} \left[1.18 \sqrt{\frac{1-\varepsilon}{3\pi}} \left(\frac{1}{1-e^{-((1-\varepsilon)/0.04)}} \right) \right]^{-1.11} \quad (9)$$

$$C = 0.00212(1-\varepsilon)^{-0.132} \left[1.18 \sqrt{\frac{1-\varepsilon}{3\pi}} \left(\frac{1}{1-e^{-((1-\varepsilon)/0.04)}} \right) \right]^{-1.63} \quad (10)$$

For the one-temperature model, the effective thermal conductivities of composite PCMs are an indispensable parameter to numerically simulate phase change heat transfer. Many models are employed to determine the effective thermal conductivities, which are proposed in previous literature. The theoretical model developed by Bhattacharya et al. [33] is very close to actual configuration of metal foam. Thus, Bhattacharya's model is employed in the present study. The effective thermal conductivity can be defined as:

$$k_{eff} = 0.35(\varepsilon k_f + (1-\varepsilon)k_s) + \frac{0.65}{\left(\frac{\varepsilon}{k_f} + \frac{1-\varepsilon}{k_s}\right)} \quad (11)$$

3.3 Initial and boundary conditions

The initial velocity for solid PCM is zero, and the initial temperature is at a constant temperature of 298K, the initial condition can be given by:

$$0 \leq x \leq 50, 0 \leq y \leq 50, u=v=0, T_i=298K \quad (12)$$

The boundary conditions required for governing equations can be also found in Fig. 3 and defined by the following equations:

$$x=0, 0 \leq y \leq 50, u=v=0, T_w=350K \quad (13)$$

$$x=50, 0 \leq y \leq 50, u=v=0, \frac{\partial T}{\partial x} = 0 \quad (14)$$

$$y=0, 0 \leq x \leq 50, u=v=0, \frac{\partial T}{\partial y} = 0 \quad (15)$$

$$y=50, 0 \leq x \leq 50, u=v=0, \frac{\partial T}{\partial y} = 0 \quad (16)$$

3.4 Numerical procedure and validation

For the present numerical simulation, commercial CFD software FLUENT 18.0 is adopted to solve the governing equations along with the initial and boundary conditions based on finite volume method. The second order upwind differencing scheme is recommended to discretize the governing equation for momentum and energy. PRESTO is applied to compute the pressure equation, which is recommended to calculate the liquid flow within the porous medium. PISO algorithm is used for coupling velocity-pressure field. The convergence of

solution is checked at every time step for numerical simulation at unsteady state, and the convergence criteria of scaled residual are set to 10^{-6} to monitor calculation stability of energy and momentum equations. Structure grids are generated in the computational domain of the two-dimension model. The grid and time independence tests are performed for guaranteeing the validity of numerical simulation. Three different numbers of grids (43k, 63k and 77k cells) and three different time steps (0.5 s, 1 s and 2 s) are examined. The liquid fraction of composite PCM with Cond.1 is tested using the above three grids and time steps. The comparison results are presented in Fig. 4(a) and (b). It is observed that results exhibit good agreement and the relative error is within 2%. To ensure the calculation accuracy and reduce computation time, the medial grid 63k cells and time step 1 s are enough for present numerical simulation.

The model in the present study is validated with the experimental results extracted in the literature. The same copper foam and paraffin is used in numerical simulation for comparison with Zheng et al. [34], and the same initial and boundary condition is adopted. The evolvement comparison of solid-liquid interface is exhibited in Fig. 5. Blue represents solid phase for composite PCM. It can be found that the numerical results are good in agreement with experimental photos. Hence, the present model can be applied to numerically simulate phase change heat transfer of copper foam saturated with paraffin.

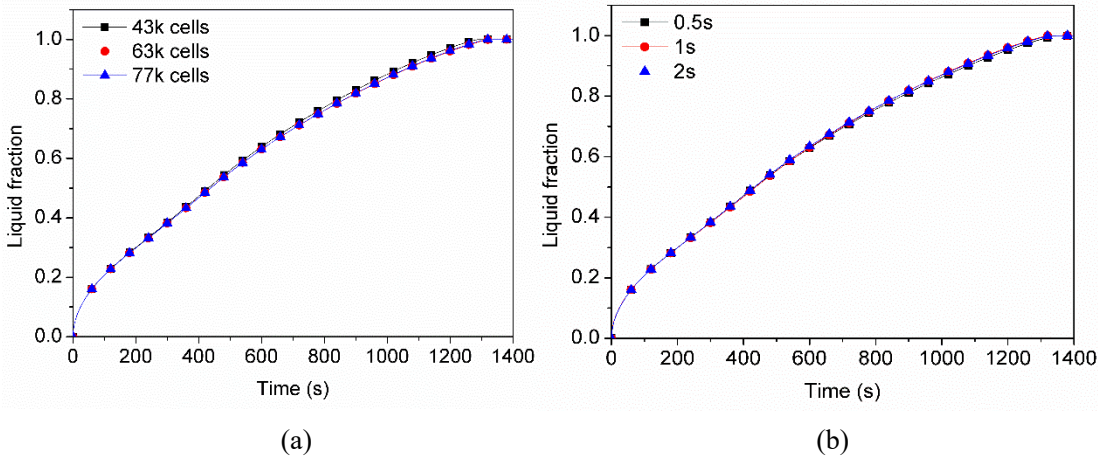


Fig. 4. Independence tests of (a) grids and (b) time step

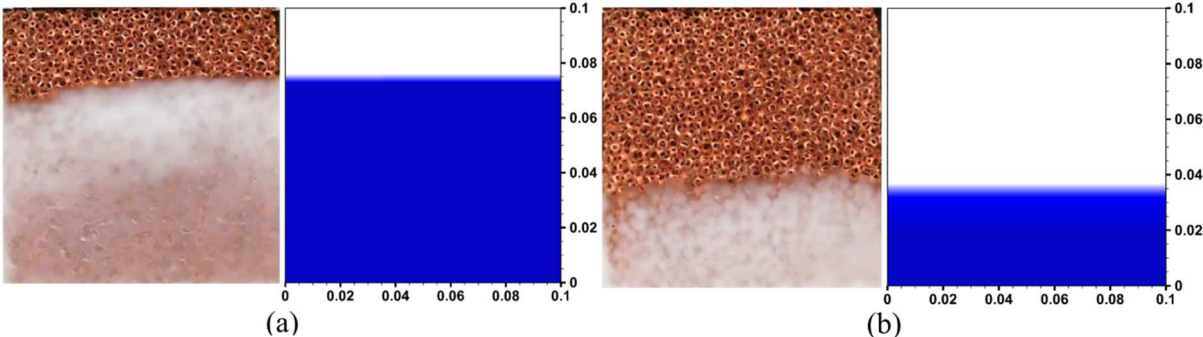


Fig. 5. Comparison of numerical results and experimental data. (a) at $t = 3h$, (b) at $t = 4.5h$

4. Results and discussion

4.1 Evolvement of phase change charging

Fig. 6 shows the evolution of phase change of composite PCM under Conds. 1-3. The solid-liquid interface contours for every condition are extracted at 20%, 40% and 80% liquid fraction, respectively. The solid-liquid interfaces are flat and parallel with the top face, which indicates that natural convection within composite PCM is distinctly suppressed under top heating condition. The numerical results of Hu et al. [35] also showed the flat melting interface, which indicated that heat transfer of composite PCM with top heating was dominated by heat conduction. It can be found that the velocity value is very small (order of magnitude 10^{-6}) and can be almost ignored during the melting process, which also demonstrates that natural convection of liquid PCM is restrained and heat conduction dominates heat transfer during the whole phase change process. The melting time of composite PCMs is almost the same at the same liquid fraction.

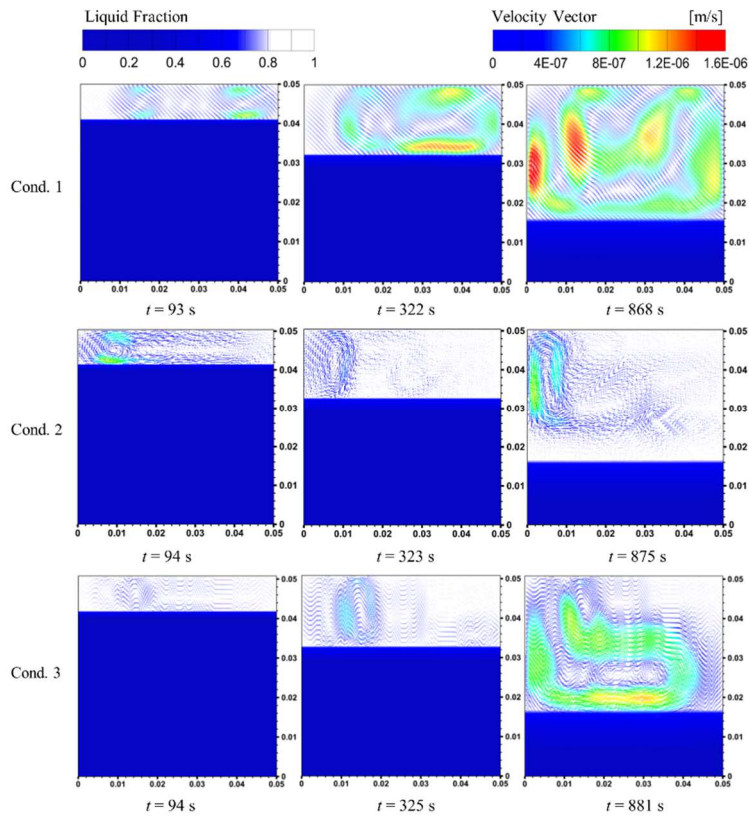


Fig. 6. Evolution of phase change for composites with top heating at 20%, 40% and 80% liquid fraction

Fig. 7 presents the evolution of phase change of composite PCM under Conds. 4-6. The solid-liquid interface is mildly inclined at the initial stage of melting, which owes to the effect of natural convection. As melting progresses, liquid paraffin flows upward and collides with solid paraffin at the interface location. It is noted from the vector diagrams that the velocity value is the greater close to hot face and interface during phase change process. The melting for PCM within top region is quicker than bottom region and melting interface is inclined, which is ascribed to role of natural convection. This indicates that natural convection plays a dominant role in phase change heat transfer. It is noted that the velocity decreases with the increase of contact gap at the same liquid fraction. This phenomenon demonstrates that natural convection can be restrained as contact conditions grow worse (i.e. the gap size increases). As a result, the melting time is longer for the larger contact gap when the liquid

fraction is the same, e.g., the melting time of Cond. 6 is 1387s and almost prolonged about 2.8 times as much as that of Cond. 4 at the 80% liquid fraction.

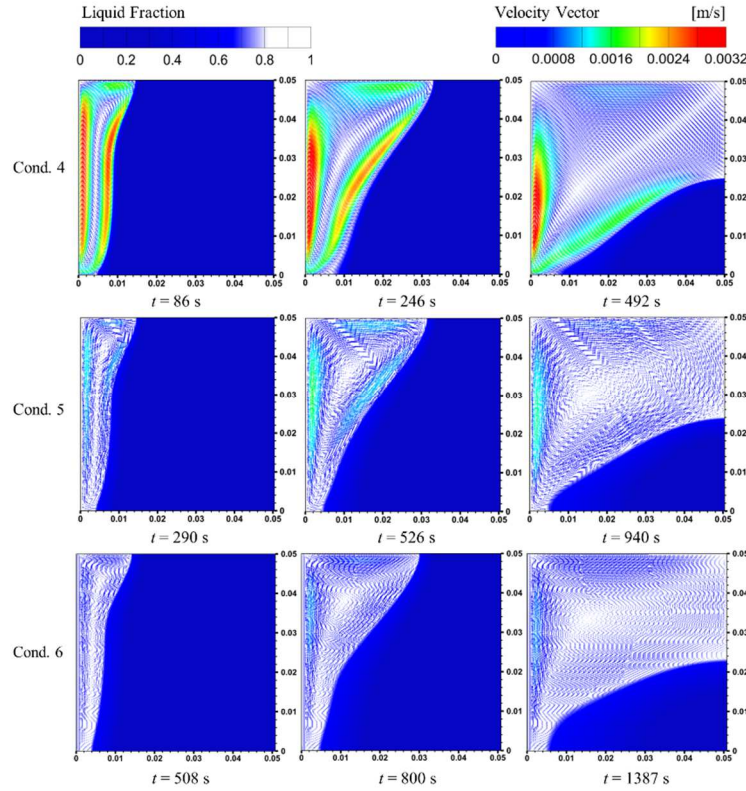


Fig. 7. Evolvement of phase change for composites with left heating at 20%, 40% and 80% liquid fraction

Fig. 8 shows the evolvement of phase change for composites under Conds. 7-9. At the beginning of melting process, the solid-liquid interface is flat and parallel to bottom face. Moreover, velocity is extremely weak in the liquid phase domain. It reveals that heat conduction is in a dominant position at the early period of phase transition. As melting continues, solid-liquid interface is wavy, which is attributed to the influence of natural convection. It can be found from experimental results of Yang et al. [36] that a similar phenomenon was showed in melting evolution of composite PCM with bottom heating (i.e. there is a wavy melting interface). It is demonstrated that the heat conduction and natural convection have comprehensive influences on thermal charging process. It can be seen that the melting of composites in the middle region is quicker than other regions and the velocity gradually increases, which confirms that natural convection becomes stronger and gradually dominates the melting process of composites in the late stage of melting. We can find from the velocity vector diagrams that velocity declines with the increase of contact gap. As a consequence, melting time of composites with the larger contact gap is lengthened at the same liquid fraction, which is owing to the influence of contact condition on natural convection.

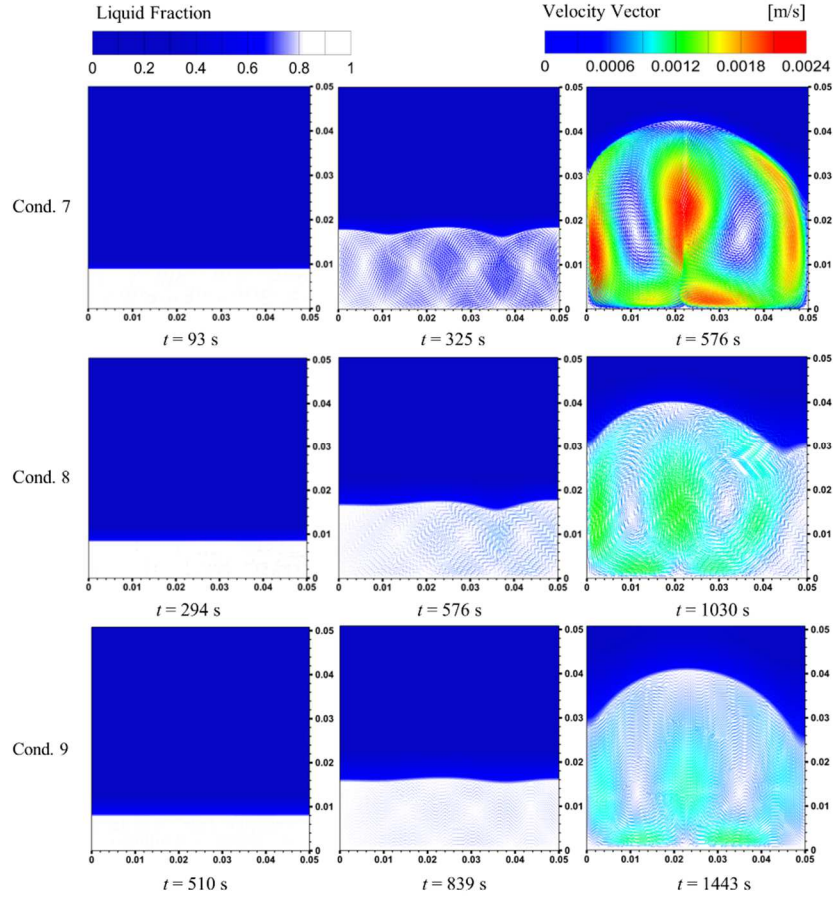


Fig. 8. Evolvement of phase change for composites with bottom heating at 20%, 40% and 80% liquid fraction

To study the influence of heating condition, numerical results of Conds. 1, 4 and 7 are compared and analyzed. It can be found that heat transfer mechanism is significantly different under different heating conditions, e.g., heat conduction dominates the thermal charging process under top heating condition, whereas natural convection plays a dominant role in phase transition heat transfer under left heating condition. The melting time of composites under three heating conditions is different when liquid fraction is the same. For instance, the melting time of composite with left heating is the shortest and reduced by about 43% compared to composite with top heating, which indicates that the natural convection conduces to the enhancement of thermal charging performance of composite PCM. It is concluded that heating condition has an obvious influence on thermal charging performance by affecting phase change heat transfer mode.

4.2 Liquid fraction and melting time

The variation of liquid fraction of composites with 0 mm gap under three heating conditions is analyzed as shown in Fig. 9. It is observed from liquid fraction curves that the melting rate of composite with left heating is the fastest and almost remains the value until the end of phase transition. In addition, it can be found that the melting rate of composite under the top and bottom heating conditions is almost the same in the initial period of phase change. The melting rate for top heating is nearly invariable in the whole melting process, since

natural convection is suppressed and heat conduction dominates heat transfer as mentioned before. Whereas, the melting rate for bottom heating is visibly heightened, which results from the occurrence of natural convection in the mid stage of melting process.

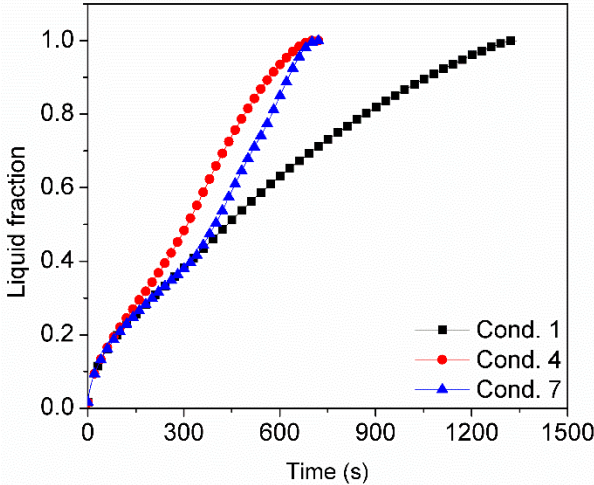


Fig. 9. Variation of liquid fraction under three heating conditions

Fig.10 presents the variation of liquid fraction of composites with left heating under three contact conditions. It is noted that the liquid fraction curves for different contact conditions show a similar variation tendency but different slope (i.e. melting rate). For example, the melting rate of composite PCM with ideal contact condition (i.e. gap is 0 mm) is the fastest and 2.6 times of that with contact gap of 0.8 mm. Furthermore, results show that the melting rate of composites decreases as contact condition worsens, which owes to additional thermal resistance caused by the contact gap between the composite PCM and hot wall.

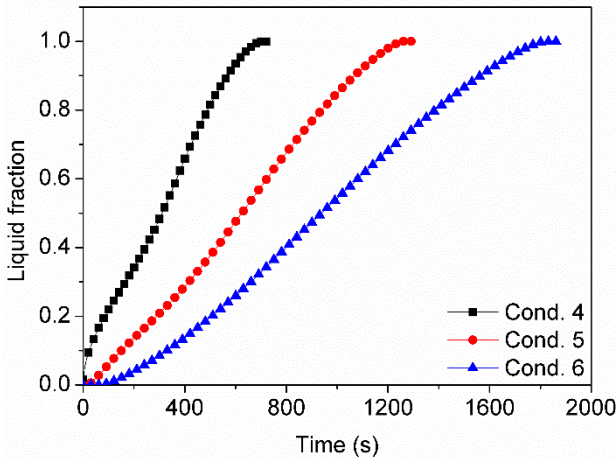


Fig . 10. Variation of liquid fraction under three contact conditions

The total melting time of composite PCMs with nine different conditions is presented in Fig. 11. The total melting time for left and bottom heating presents a linear increase with the contact gap. Whereas, the total melting time of composite for top heating hasn't a visible change with the contact gap. This phenomenon is because contact thermal resistance increases

with contact gap between composite and wall but the contact resistance can be ignored compared to thermal material resistance of composite PCM. Hence, the poor contact condition has a very small effect on thermal behavior of composite in which heat transfer is dominated by heat conduction. For the ideal contact condition (i.e. $\delta = 0$ mm), the total time is almost the same for left and bottom heating conditions, which is almost cut in half compared with top heating condition. This phenomenon is attributed to different heat transfer mode induced by the heating condition. For instance, natural convection dominates heat transfer of composite under left heating condition, which conducive to the improvement of thermal behavior, whereas, natural convection is restrained for top heating in the whole melting process, as analyzed in Section 4.1.

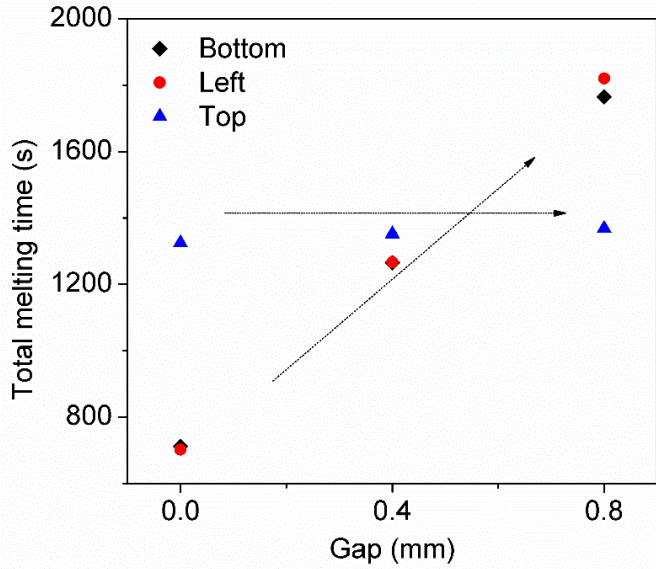


Fig. 11. Total melting time of composite PCM

4.3 Heat storage rate

The heat storage rate is a vital criterion for estimating thermal charging performance of composite PCMs. Hence, we perform the study of average heat storage rate (i.e. per unit time per unit mass of composite PCM stores energy during the whole melting process). Fig. 12 displays the average heat storage rate of composite PCM under nine different conditions. Results show that the heat storage rate of composite with left heating is the largest under the ideal contact condition (i.e. $\delta = 0$ mm), which is almost twice of that with top heating. The heat storage rate of composite with left and bottom heating visibly decreases with the increase of contact gap. In contrast, the heat storage rate of composite under top heating condition hasn't the evident reduction with the increase of contact gap. Furthermore, it is seen that the average heat storage rate of composite with top heating is larger than that with left and bottom heating under the worse contact condition (i.e. $\delta = 0.8$ mm). It is demonstrated from the above results that the effects of heating and contact conditions on thermal charging performance are significant and integrated.

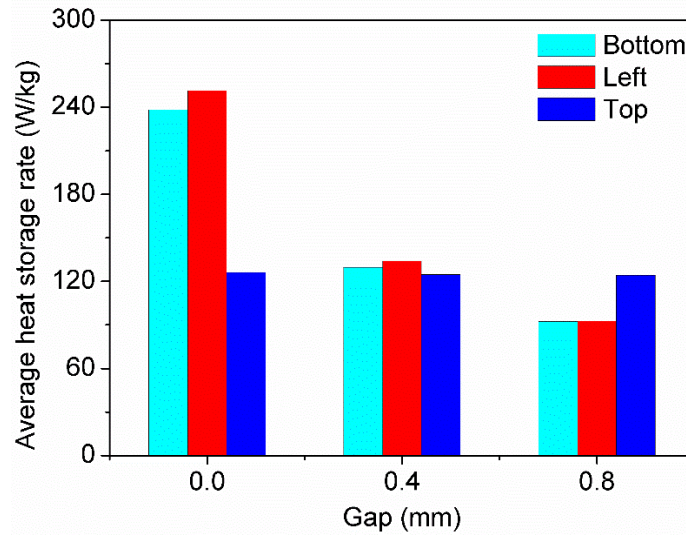


Fig. 12. Average heat storage rate

5 Conclusion

In this paper, the numerical investigation is conducted to examine the effects of heating and contact conditions on thermal charging performance of composite PCM. A two-dimensional model based on volume-averaged method is built to investigate heat transfer mechanism of composite PCM in the melting process. Nine different cases are designed to compare the effect of heating and contact conditions on thermal characteristic. The following conclusions can be extracted:

(1) The effect of heating condition can be investigated under the same contact condition. It is found from numerical results that natural convection is suppressed in the whole thermal charging process for top heating. In contrast, the natural convection plays a dominant role in heat transfer for left and bottom heating. It is demonstrated that the heat transfer mechanism is different under different heating conditions, which results in a remarkable impact on thermal charging performance of composite PCM. For instance, the total melting time of left and bottom heating is almost the same and shorten by about 50% compared to top heating when the contact gap is 0 mm.

(2) The contact condition has a significant impact upon thermal performance of composite PCM under left and bottom heating conditions, e.g., the total melting time for left and bottom heating presents a linear increase versus the contact gap. It is further confirmed that contact condition has an obvious influence on thermal characteristic of composite PCM in which heat transfer is dominated by natural convection. Conversely, the influence of contact condition under top heating condition is very small, e.g., the total melting time for top heating is almost the same under three contact conditions (i.e. contact gap is 0, 0.4 and 0.8 mm), which indicates that the influence of contact condition on thermal behavior of composite PCM (in which heat transfer is dominated by heat conduction) can be neglected and it is not necessary for metal foam to be bonded to the container wall via brazing, sintering, etc.

(3) It is found from numerical results that the heating and contact conditions have a

combined effect on the thermal charging performance of composite PCM. The heat storage rate of left and bottom heating is almost the same and higher than that of top heating when the contact condition is good (i.e. $\delta = 0$ mm). Hence, left and bottom heating are recommended in the practical application of TES due to the high heat storage rate. The heat storage rate of three heating conditions is almost the same under middle contact condition (i.e. $\delta = 0.4$ mm). Whereas, the heat storage rate of top heating is higher than that of left and bottom heating as contact condition grows worse (i.e. $\delta = 0.8$ mm).

(4) This study can provide theoretical guidance for the selection of heating and contact conditions of thermal storage system using composite PCM, such as solar thermal storage, latent heat storage device and thermal battery for taking advantage of off-peak electricity. For future work, the experimental investigation will be conducted to study the effects of contact and heating conditions on thermal charging performance of composite PCM, and optimized design of TES device using composite PCM will be performed considering role of heating and contact conditions.

Acknowledgements

The authors thank China Scholarship Council (CSC) for providing a scholarship to conduct this study.

References

- [1] A. Sharma, V.V. Tyagi, C.R. Chen, D. Buddhi, Review on thermal energy storage with phase change materials and applications, *Renew Sust Energ Rev* 13 (2009) 318-345.
- [2] E. Oro, A. de Gracia, A. Castell, M.M. Farid, L.F. Cabeza, Review on phase change materials (PCMs) for cold thermal energy storage applications, *Appl. Energy*. 99 (2012) 513-533.
- [3] K.S. Reddy, V. Mudgal, T.K. Mallick, Review of latent heat thermal energy storage for improved material stability and effective load management, *J. Energy Storage* 15 (2018) 205-227.
- [4] X. Yang, P. Wei, X. Cui, L. Jin, Y.-L. He, Thermal response of annuli filled with metal foam for thermal energy storage: An experimental study, *Appl. Energy*. 250 (2019) 1457-1467.
- [5] M.M.A. Khan, N.I. Ibrahim, I.M. Mahbubul, H.M. Ali, R. Saidur, F.A. Al-Sulaiman, Evaluation of solar collector designs with integrated latent heat thermal energy storage: A review, *Sol. Energy*. 166 (2018) 334-350.
- [6] A. de Gracia, L.F. Cabeza, Phase change materials and thermal energy storage for buildings, *Energy and Buildings* 103 (2015) 414-419.
- [7] L. Miro, J. Gasia, L.F. Cabeza, Thermal energy storage (TES) for industrial waste heat (IWH) recovery: A review, *Appl. Energy*. 179 (2016) 284-301.
- [8] C.Y. Zhao, G.H. Zhang, Review on microencapsulated phase change materials (MEPCMs): Fabrication, characterization and applications, *Renew Sust Energ Rev* 15 (2011) 3813-3832.
- [9] S. Marchi, S. Pagliolico, G. Sassi, Characterization of panels containing micro-encapsulated Phase Change Materials, *Energy Convers. Manage.* 74 (2013)

261-268.

- [10] D. Zou, X. Ma, X. Liu, P. Zheng, Y. Hu, Thermal performance enhancement of composite phase change materials (PCM) using graphene and carbon nanotubes as additives for the potential application in lithium-ion power battery, *Int. J. Heat Mass Transfer* 120 (2018) 33-41.
- [11] Q. Zhang, Z. Luo, Q. Guo, G. Wu, Preparation and thermal properties of short carbon fibers/erythritol phase change materials, *Energy Convers. Manage.* 136 (2017) 220-228.
- [12] X. Hu, X. Gong, Pore-scale numerical simulation of the thermal performance for phase change material embedded in metal foam with cubic periodic cell structure, *Appl. Therm. Eng.* 151 (2019) 231-239.
- [13] A. Arshad, H.M. Ali, M. Ali, S. Manzoor, Thermal performance of phase change material (PCM) based pin-finned heat sinks for electronics devices: Effect of pin thickness and PCM volume fraction, *Appl. Therm. Eng.* 112 (2017) 143-155.
- [14] C.Y. Zhao, W. Lu, Y. Tian, Heat transfer enhancement for thermal energy storage using metal foams embedded within phase change materials (PCMs), *Sol. Energy.* 84 (2010) 1402-1412.
- [15] W.Q. Li, Z.G. Qu, Y.L. He, W.Q. Tao, Experimental and numerical studies on melting phase change heat transfer in open-cell metallic foams filled with paraffin, *Appl. Therm. Eng.* 37 (2012) 1-9.
- [16] X. Hu, F. Zhu, X. Gong, Experimental and numerical study on the thermal behavior of phase change material infiltrated in low porosity metal foam, *J. Energy Storage* 26 (2019) 101005.
- [17] X. Yang, J. Yu, Z. Guo, L. Jin, Y.-L. He, Role of porous metal foam on the heat transfer enhancement for a thermal energy storage tube, *Appl. Energy.* 239 (2019) 142-156.
- [18] X. Yang, J. Yu, T. Xiao, Z. Hu, Y.-L. He, Design and operating evaluation of a finned shell-and-tube thermal energy storage unit filled with metal foam, *Appl. Energy.* 261 (2020) 114385.
- [19] X. Xiao, P. Zhang, M. Li, Effective thermal conductivity of open-cell metal foams' impregnated with pure paraffin for latent heat storage, *International Journal of Thermal Sciences* 81 (2014) 94-105.
- [20] X. Xiao, P. Zhang, M. Li, Preparation and thermal characterization of paraffin/metal foam composite phase change material, *Appl. Energy.* 112 (2013) 1357-1366.
- [21] K. Lafdi, O. Mesalhy, S. Shaikh, Experimental study on the influence of foam porosity and pore size on the melting of phase change materials, *J. Appl. Phys.* 102 (2007).
- [22] X. Yang, W. Wang, C. Yang, L. Jin, T.J. Lu, Solidification of fluid saturated in open-cell metallic foams with graded morphologies, *Int. J. Heat Mass Transfer* 98 (2016) 60-69.
- [23] J.L. Yang, L.J. Yang, C. Xu, X.Z. Du, Numerical analysis on thermal behavior of solid-liquid phase change within copper foam with varying porosity, *Int. J. Heat Mass Transfer* 84 (2015) 1008-1018.
- [24] R. Baby, C. Balaji, Experimental investigations on thermal performance enhancement and effect of orientation on porous matrix filled PCM based heat sink, *International Communications in Heat and Mass Transfer* 46 (2013) 27-30.
- [25] P. Zhang, Z.N. Meng, H. Zhu, Y.L. Wang, S.P. Peng, Melting heat transfer characteristics

- of a composite phase change material fabricated by paraffin and metal foam, *Appl. Energy*. 185 (2017) 1971-1983.
- [26] H.-Q. Jin, L.-W. Fan, M.-J. Liu, Z.-Q. Zhu, Z.-T. Yu, A pore-scale visualized study of melting heat transfer of a paraffin wax saturated in a copper foam: Effects of the pore size, *Int. J. Heat Mass Transfer* 112 (2017) 39-44.
- [27] K. Boomsma, D. Poulikakos, On the effective thermal conductivity of a three-dimensionally structured fluid-saturated metal foam, *Int. J. Heat Mass Transfer* 44 (2001) 827-836.
- [28] S.S. Feng, M. Shi, Y.F. Li, T.J. Lu, Pore-scale and volume-averaged numerical simulations of melting phase change heat transfer in finned metal foam, *Int. J. Heat Mass Transfer* 90 (2015) 838-847.
- [29] A. Yataganbaba, I. Kurtbas, Effect of Heating Position on Thermal Energy Storage in Cavity With/Without Open-cell Metallic Foams, *Experimental Heat Transfer* 29 (2016) 355-377.
- [30] G. Ferrer, A. Solé, C. Barreneche, I. Martorell, L.F. Cabeza, Corrosion of metal containers for use in PCM energy storage, *Renewable Energy* 76 (2015) 465-469.
- [31] ANSYS fluent software package: user's manual, 18.0, 2017.
- [32] V.V. Calmidi, *Transport Phenomena in High Porosity Fibrous Metal Foams*, University of Colorado, 1998.
- [33] A. Bhattacharya, V.V. Calmidi, R.L. Mahajan, Thermophysical properties of high porosity metal foams, *Int. J. Heat Mass Transfer* 45 (2002) 1017-1031.
- [34] H. Zheng, C. Wang, Q. Liu, Z. Tian, X. Fan, Thermal performance of copper foam/paraffin composite phase change material, *Energy Convers. Manage.* 157 (2018) 372-381.
- [35] X. Hu, S.S. Patnaik, Modeling phase change material in micro-foam under constant temperature condition, *Int. J. Heat Mass Transfer* 68 (2014) 677-682.
- [36] X.H. Yang, Z.X. Guo, Y.H. Liu, L.W. Jin, Y.L. He, Effect of inclination on the thermal response of composite phase change materials for thermal energy storage, *Appl. Energy*. 238 (2019) 22-33.